J|A|C|S
ARTICLES
Published on Web 04/12/2007

Infrared Spectroscopy and Theoretical Studies on Gas-Phase Protonated Leu-enkephalin and Its Fragments: Direct Experimental Evidence for the Mobile Proton

Nick C. Polfer,*,† Jos Oomens,† Sándor Suhai,‡ and Béla Paizs*,‡

Contribution from the FOM Institute for Plasma Physics "Rijnhuizen", Edisonbaan 14, NL-3439 MN Nieuwegein, The Netherlands, and German Cancer Research Center, Im Neuenheimer Feld 580, D-69120 Heidelberg, Germany

Received November 14, 2006; E-mail: polfer@rijnh.nl; b.paizs@dkfz.de

Abstract: The gas-phase structures of the protonated pentapeptide Leu-enkephalin and its main collision-induced dissociation (CID) product ions, b_4 and a_4, are investigated by means of infrared multiple-photon dissociation (IR-MPD) spectroscopy and detailed molecular mechanics and density functional theory (DFT) calculations. Our combined experimental and theoretical approach allows accurate structural probing of the site of protonation and the rearrangement reactions that have taken place in CID. It is shown that the singly protonated Leu-enkephalin precursor is protonated on the N-terminus. The b_4 fragment ion forms two types of structures: linear isomers with a C-terminal oxazolone ring, as well as cyclic peptide structures. For the former structure, two sites of proton attachment are observed, on the N-terminus and on the oxazolone ring nitrogen, as shown in a previous communication (Polfer, N. C.; Oomens, J.; Suhai, S.; Paizs, B. *J. Am. Chem. Soc.* **2005**, *127*, 17154−17155). Upon leaving the ions for longer radiative cooling delays in the ion cyclotron resonance (ICR) cell prior to IR spectroscopic investigation, one observes a gradual decrease in the relative population of oxazolone-protonated b_4 and a corresponding increase in N-terminal-protonated b_4. This experimentally demonstrates that the mobile proton is transferred between two sites in a gas-phase peptide ion and allows one to rationalize how the proton moves around the molecule in the dissociation process. The a_4 fragment, which is predominantly formed via b_4, is also confirmed to adopt two types of structures: linear imine-type structures, and cyclic structures; the former isomers are exclusively protonated on the N-terminus in sharp contrast to b_4, where a mixture of protonation sites was found. The presence of cyclic b_4 and a_4 fragment ions is the first direct experimental proof that fully cyclic structures are formed in CID. These results suggest that their presence is significant, thus lending strong support to the recently discovered peptide fragmentation pathways (Harrison, A. G.; Young, A. B.; Bleiholder, B.; Suhai, S.; Paizs, B. *J. Am. Chem. Soc.* **2006**, *128*, 10364−10365) that result in scrambling of the amino acid sequence upon CID.

Introduction

Mass spectrometry is becoming increasingly important in the life sciences due to its high sensitivity, high information content, and ability to study complex mixtures. Peptide tandem mass spectrometry[1−3] (MS/MS) with the aim of determining the amino acid sequence of peptides is in fact the key technology for protein identification in the rapidly expanding field of proteomics.[4,5] The most common instruments utilize collision-induced dissociation (CID) of protonated peptides, where collisions with a neutral background gas induce bond cleavages in the molecule. Under low collision energy conditions, protonated peptides predominantly fragment to produce so-called N-terminal *b* and C-terminal *y* fragment ions.[6,7] Despite great instrumental advances in the automation of MS/MS of peptides, the correct interpretation of CID spectra is often complicated by incomplete sequence coverage and/or unusual dissociation processes. Current database search algorithms that make use of tandem mass spectra, such as SEQUEST[8] and Mascot,[9] mainly make use of the fragment masses, while neglecting their intensities. It is widely accepted in the peptide-sequencing community that the interpretation of CID spectra could be much improved by incorporating mechanistic information on the peptide fragmentation pathways (PFP's).[10] This, however, requires a thorough understanding of the underlying dissociation chemistry.

† FOM Institute for Plasma Physics "Rijnhuizen".
‡ German Cancer Research Center.

(1) McLafferty, F. W. *Tandem Mass Spectrometry*; Wiley-Interscience: New York, 1983.
(2) Hunt, D. F.; Yates, J. R., III; Shabanovitz, J.; Winston, S.; Hauer, C. R. *Proc. Natl. Acad. Sci. U.S.A.* **1986**, *83*, 6233.
(3) Biemann, K.; Scoble, H. A. *Science* **1987**, *237*, 992.
(4) Aebersold, R.; Goodlett, D. R. *Chem. Rev.* **2001**, *101*, 269.
(5) Steen, H.; Mann, M. *Nat. Rev. Mol. Cell Biol.* **2004**, *5*, 699.
(6) Roepstorff, P.; Fohlmann, J. *J. Biomed. Mass Spectrom.* **1984**, *11*, 601.
(7) Biemann, K. *Biomed. Environ. Mass Spectrom.* **1988**, *16*, 99.
(8) Eng, J. K.; McCormack, A. L.; Yates, J. R., III. *J. Am. Soc. Mass Spectrom.* **1994**, *5*, 976.
(9) Perkins, D. N.; Pappin, D. J. C.; Creasy, D. M.; Cottrell, J. S. *Electrophoresis* **1999**, *20*, 3551.
(10) Paizs, B.; Suhai, S. *Mass Spectrom. Rev.* **2005**, *24*, 508.

10.1021/ja068014d CCC: $37.00

The first peptide fragmentation model that attempted to explain the dissociation chemistry of protonated peptides was the mobile proton model.[11,12] In the framework of this model, the extra proton is transferred upon excitation from an unreactive site of higher gas-phase basicity (e.g., Arg or Lys side chain or the N-terminal amino group) to form energetically less favored but reactive backbone amide-protonated species. Protonation on the amide nitrogen leads to considerable weakening of the amide bond,[13] and the related species play a critical role in most of the PFP's[10] that lead to sequence-informative *b*, *a*, and *y* fragments. The mobile proton model is based on a broad range of empirical peptide dissociation[14−26] and modeling[27−29] studies. It allows one to predict whether a given peptide in a particular protonation state is expected to produce sequence-informative tandem mass spectra, or whether selective cleavage at some amide bonds hinders MS-based peptide sequencing.[30] For example, peptide ions where the number of added protons exceeds the number of Arg and Lys residues are expected to fragment at various amide bonds, producing sequence-informative MS/MS spectra. On the other hand, poor sequence coverage is expected if the number of added protons equals the number of Arg residues, especially if the peptide contains Asp or Glu residues, as cleavage C-terminal to these residues (aspartic acid effect) is mainly observed. Nevertheless, the mobile proton model cannot give an accurate prediction of the relative intensities of fragment ions, for which a deeper understanding of peptide dissociation is necessary.

The recently introduced pathways in competition (PIC) model[10] provide a general framework to understand gas-phase peptide chemistry, taking into account specific features of individual peptide fragmentation pathways and their interaction. The PIC model predicts that fragment ion abundances in the MS/MS spectra of peptides are determined by pre-cleavage, amide bond-cleavage, and post-cleavage events. The pre-cleavage phase involves proton-transfer reactions and/or internal rotations necessary to produce fragmenting species. The activity or inactivity of proton-transfer pathways is the main tenet of the mobile proton model, and the related predictive rules (see above) are directly incorporated into PIC. In other words, PIC is a logical extension to the mobile proton model that considers not only the initial proton transfer but also other reactions to explain fragment ion abundances in the tandem mass spectra of peptides.

A plethora of PFP's can be envisaged that lead to sequence informative *b*, *a*, and *y* fragments of protonated peptides. Recent studies indicate, however, that only a handful of these PFP's are indeed active.[10,31] The mechanism, energetics, and kinetics of the b_n-y_m,[32−34] a_n-y_m, and side-chain nucleophile activated PFP's are already well-known or the subject of recent detailed studies. PIC pays significant attention to the post-cleavage phase of peptide fragmentation that attracted surprisingly limited research activity in the past. The fate of the added proton, that is, which fragment survives the dissociation as the charged species, can often be predicted considering fragment proton affinities (or gas-phase basicities).[35]

In a recent paper, we have shown that the fragments kept together in proton-bound dimers can undergo various transitions including association reactions and further dissociation of the reorganized parent ion.[36] Furthermore, it was shown that linear *b* ions with a C-terminal oxazolone ring can rearrange to form a cyclic peptide isomer,[31] the fragmentation of which could lead to scrambling of the primary sequence information. Related fragments have been termed non-direct sequence ions.[31] The flexibility of PIC enables us to understand the rather rich chemistry of the post-cleavage phase of peptide fragmentation that is not addressed by the mobile proton model.

Some of the current limitations to the understanding of peptide dissociation mechanisms arise from the fact that the theoretically predicted mechanisms and structures are difficult to validate with experimental approaches. In particular, very few experimental methods allow one to directly identify (1) the chemical structure and (2) the protonation site(s) of peptide fragment ions. Infrared spectroscopy has in recent years been shown to give detailed chemical information on ionic biomolecules in mass spectrometry, such as the location of proton attachment,[37,38] the zwitterionic nature of amino acids and peptides,[39−41] the binding geometry of amino acids around transition metals,[42] and the reaction products of gas-phase H/D exchange.[43] Recently, we have demonstrated the powerful use of IR spectroscopy for the structural identification of CID product ions, by experimentally

(11) Dongre, A. R.; Jones, L. I.; Somogyi, A.; Wysocki, V. H. *J. Am. Chem. Soc.* **1996**, *118*, 8365.
(12) Wysocki, V. H.; Tsaprailis, G.; Smith, L. L.; Breci, L. A. *J. Mass Spectrom.* **2000**, *35*, 1399.
(13) Somogyi, A.; Wysocki, V. H.; Mayer, I. *J. Am. Soc. Mass Spectrom.* **1994**, *5*, 704.
(14) Biemann, K.; Martin, S. A. *Mass Spectrom. Rev.* **1987**, *6*, 1.
(15) Poulter, L.; Taylor, L. C. E. *Int. J. Mass Spectrom. Ion Processes* **1989**, *91*, 183.
(16) Burlet, O.; Yang, C. Y.; Gaskell, S. J. *J. Am. Soc. Mass Spectrom.* **1992**, *3*, 337.
(17) Tang, X.; Boyd, R. K. *Rapid Commun. Mass Spectrom.* **1992**, *6*, 651.
(18) Burlet, O.; Orkiszewski, R. S.; Ballard, K. D.; Gaskell, S. J. *Rapid Commun. Mass Spectrom.* **1992**, *6*, 658.
(19) McCormack, A. L.; Somogyi, A.; Dongre, A. R.; Wysocki, V. H. *Anal. Chem.* **1993**, *65*, 2859.
(20) Tang, X.-J.; Thibault, P.; Boyd, R. K. *Anal. Chem.* **1993**, *65*, 2824.
(21) Johnson, R. S.; Krylov, D.; Walsh, K. A. *J. Mass Spectrom.* **1995**, *30*, 386.
(22) Nold, M. J.; Wesdemiotis, C.; Yalcin, T.; Harrison, A. G. *Int. J. Mass Spectrom. Ion Processes* **1997**, *164*, 137.
(23) Harrison, A. G.; Yalcin, T. *Int. J. Mass Spectrom.* **1997**, *165*, 339.
(24) Summerfield, S. G.; Whiting, A.; Gaskell, S. J. *Int. J. Mass Spectrom. Ion Processes* **1997**, *162*, 149.
(25) Harrison, A. G.; Tu, Y.-P. *J. Mass Spectrom.* **1998**, *33*, 532.
(26) Jorgensen, T. J. D.; Gardsvoll, H.; Ploug, M.; Roepstorff, P. *J. Am. Chem. Soc.* **2005**, *127*, 2785.
(27) Csonka, I. P.; Paizs, B.; Lendvay, G.; Suhai, S. *Rapid Commun. Mass Spectrom.* **2000**, *14*, 417.
(28) Paizs, B.; Csonka, I. P.; Lendvay, G.; Suhai, S. *Rapid Commun. Mass Spectrom.* **2001**, *15*, 637.
(29) Csonka, I. P.; Paizs, B.; Lendvay, G.; Suhai, S. *Rapid Commun. Mass Spectrom.* **2001**, *15*, 1457.
(30) Tsaprailis, G.; Nair, H.; Somogyi, A.; Wysocki, V. H.; Zhong, W.; Futrell, J. H.; Summerfield, S. G.; Gaskell, S. J. *J. Am. Chem. Soc.* **1999**, *121*, 5142.
(31) Harrison, A. G.; Young, A. B.; Bleiholder, B.; Suhai, S.; Paizs, B. *J. Am. Chem. Soc.* **2006**, *128*, 10364.
(32) Paizs, B.; Suhai, S. *Rapid Commun. Mass Spectrom.* **2001**, *15*, 2307.
(33) Paizs, B.; Suhai, S. *Rapid Commun. Mass Spectrom.* **2002**, *16*, 1699.
(34) Paizs, B.; Suhai, S. *J. Am. Soc. Mass Spectrom.* **2004**, *15*, 103.
(35) Harrison, A. G.; Young, A. B. *J. Am. Soc. Mass Spectrom.* **2004**, *15*, 1810.
(36) Cooper, T.; Talaty, E.; Grove, J.; Suhai, S.; Paizs, B.; Van Stipdonk, M. J. *J. Am. Soc. Mass Spectrom.* **2006**, *17*, 1654.
(37) Lucas, B.; Gregoire, G.; Lemaire, J.; Maitre, P.; Ortega, J.-M.; Rupenyan, A.; Reimann, B.; Schermann, J.-P.; Desfrancois, C. *Phys. Chem. Chem. Phys.* **2004**, *6*, 2659.
(38) Lucas, B.; Gregoire, G.; Lemaire, J.; Maitre, P.; Glotin, F.; Schermann, J.-P.; Desfrancois, C. *Int. J. Mass Spectrom.* **2005**, *243*, 97.
(39) Kapota, C.; Lemaire, J.; Maitre, P.; Ohanessian, G. *J. Am. Chem. Soc.* **2004**, *126*, 1836.
(40) Polfer, N.; Paizs, B.; Snoek, L. C.; Compagnon, I.; Suhai, S.; Meijer, G.; von Helden, G.; Oomens, J. *J. Am. Chem. Soc.* **2005**, *127*, 8571.
(41) Kamariotis, A.; Boyarkin, O. V.; Mercier, S. R.; Beck, R. D.; Bush, M. F.; Williams, E. R.; Rizzo, T. R. *J. Am. Chem. Soc.* **2006**, *128*, 905.
(42) Polfer, N. C.; Oomens, J.; Moore, D. T.; von Helden, G.; Meijer, G.; Dunbar, R. C. *J. Am. Chem. Soc.* **2006**, *128*, 517.
(43) Polfer, N. C.; Dunbar, R. C.; Oomens, J. *J. Am. Soc. Mass Spectrom.* **2007**, *18*, 512.

showing that oxazolone ring structures are formed for the b_4 CID fragment ion of protonated Leu-enkephalin.[44] Here, we present a more extensive IR spectroscopy and theoretical study of protonated Leu-enkephalin, involving the structural investigation of the precursor ion, as well as its main CID product ions b_4 and a_4 under low-energy conditions. This peptide is in fact one of the most intensively studied systems by mass spectrometric dissociation methods and hence constitutes an excellent example for comparison.[45−57] Furthermore, in a parallel study, the PFP's of protonated Leu-enkephalin and its major fragments were extensively studied using computational and complementary experimental techniques,[58] which support the interpretation of the IR-MPD data presented here.

Experimental Section and Computations

Mass Spectrometry. All experiments were carried out at the FOM Institute for Plasma Physics "Rijnhuizen" (Nieuwegein, The Netherlands) using a laboratory-built Fourier transform ion cyclotron resonance (FT-ICR) mass spectrometer.[59] The singly protonated pentapeptide Leu-enkephalin (*m*/*z* 556) (Tyr−Gly−Gly−Phe−Leu) (Sigma Aldrich) was generated in a commercial electrospray ionization (ESI) source (Micromass, Manchester, U.K.). The peptide ions were accumulated in a hexapole trap prior to pulsed extraction via a quadrupole deflector and an rf octopole ion guide to the Penning trap. As the ions travel through the octopole, its DC bias is switched (from ground potential to typically −40 V), thereby redefining the potential energy of the ions, while leaving their kinetic energy unchanged. By means of this electrostatic pulsing method (described in detail elsewhere),[42] the ions can be stored in the ICR cell using relatively low trapping voltages without the need of a gas pulse. After a radiative cooling delay (typically 350 ms) and mass isolation, the protonated Leu-enkephalin precursor ion was irradiated with pulses (40 macropulses at 10 Hz repetition rate) from the free electron laser for infrared experiments (FELIX).[60] FELIX produces high-energy pulses (∼50 mJ) of tunable wavelength (3−250 μm) and is hence highly suited for inducing photodissociation.

In the CID experiments, the fragment ions of interest, b_4 (*m*/*z* 425) and a_4 (*m*/*z* 397), were generated by sustained off-resonance irradiation (SORI) CID (2−4 s) with a background gas (2×10^{-7} mbar). This pressure was found to be a good tradeoff between inducing abundant dissociation and maintaining reasonable ICR transients. Conversely, using a gas pulse to momentarily increase the pressure was found to be unreliable in reproducing the ion population and pressure conditions, which is essential to generate reliable IR spectra. The production of b_4 was effected by employing a low-amplitude SORI voltage on protonated Leu-enkephalin, whereas the generation of a_4 was optimized by using a slightly higher SORI voltage, as well as a simultaneous SORI pulse to dissociate b_4. Previous dissociation studies on these fragment ions have shown that the formation of a_4 requires a higher activation energy and have indicated that a_4 is predominantly formed by sequential dissociation of protonated Leu-enkephalin to b_4 followed by CO loss to produce a_4,[51,52,61] although some a_4 can also be produced directly from protonated Leu-enkephalin.[54]

IR-MPD Spectroscopy. Spectroscopy of mass-selected ions requires "action" spectroscopy approaches, as their density is too low to allow direct absorption spectroscopy. In these experiments, we made use of infrared multiple-photon dissociation (IR-MPD) spectroscopy.[62] In IR-MPD, the ion absorbs a photon when a vibrational mode of the molecule is resonant with the laser wavelength. This energy is quickly (i.e., <picoseconds) dissipated in the molecule by intramolecular vibrational redistribution (IVR), which allows absorption of another photon at the same wavelength. In this process, tens to hundreds of photons are absorbed in a resonant, yet non-coherent fashion, leading to dissociation of the ion.

The IR spectrum of the ion of interest was then recorded by monitoring its photodepletion and/or photodissociation yield as a function of wavelength (here 800−2500 cm^{-1}). In the IR-MPD study of CID fragments, the photodissociation appearance spectrum (i.e., $\sum$(photofragments)/$\sum$(all ions)) was found to be less reliable due to an apparent nonconservation of the total ion count, suggesting that some photofragments were lost from the trap, or were at least less well detected. In the corresponding IR-MPD experiments on protonated Leu-enkephalin precursor ion, where no SORI CID was carried out, this ion nonconservation problem was not observed. The discrepancy in the CID experiments could be explained by the fact that SORI CID causes the ion population to be taken away from the center of the trap, thereby resulting in less efficient trapping/detection of the photofragment ions. As the photodepletion spectra for a_4 and b_4 were highly reproducible, these give an accurate representation of the IR spectra of the ions. Moreover, the depletion and appearance IR-MPD spectra of protonated Leu-enkephalin were found to be qualitatively identical (see Figure 1A and B).

At each wavelength step, four mass spectra were averaged; five photodissociation spectra were recorded for each ion, which were then averaged to yield the final IR-MPD spectra. These spectra were also linearly normalized for the laser power over the wavelength region. It should be noted that an IR-MPD spectrum is not identical to a linear absorption spectrum, but that a linear approximation serves as a reasonably good approximation.[63] The discrepancies to an absorption spectrum include red-shifting and broadening of vibrational bands, as well as variations in intensities of adjacent bands, and have been well documented.[40,63,64] The experimental IR spectra were compared to theoretical spectra for putative calculated structures to obtain the best match.

Calculations. All calculations were performed at the German Cancer Research Institute in Heidelberg, Germany. A recently developed conformational search engine[10,34,65,66] devised to deal with protonated

(44) Polfer, N. C.; Oomens, J.; Suhai, S.; Paizs, B. *J. Am. Chem. Soc.* **2005**, *127*, 17154.
(45) Gaskell, S. J.; Reilly, M. H.; Porter, C. J. *Rapid Commun. Mass Spectrom.* **1988**, *2*, 142.
(46) Alexander, A. J.; Boyd, R. K. *Int. J. Mass Spectrom. Ion Processes* **1989**, *90*, 211.
(47) Ballard, K. D.; Gaskell, S. J. *Int. J. Mass Spectrom. Ion Processes* **1991**, *111*, 173.
(48) Bean, M. F.; Carr, S. A.; Thorne, G. C.; Reilly, M. H.; Gaskell, S. J. *Anal. Chem.* **1991**, *63*, 1473.
(49) Meot-Near, M.; Dongree, A. R.; Somogyi, A.; Wysocki, V. H. *Rapid Commun. Mass Spectrom.* **1995**, *9*, 829.
(50) Vekey, K.; Somogyi, A.; Wysocki, V. H. *J. Mass Spectrom.* **1995**, *30*, 212.
(51) Schnier, P. D.; Price, W. D.; Strittmatter, E. F.; Williams, E. R. *J. Am. Soc. Mass Spectrom.* **1997**, *8*, 771.
(52) Vachet, R. W.; Bishop, B. M.; Erickson, B. W.; Glish, G. L. *J. Am. Chem. Soc.* **1997**, *119*, 5481.
(53) Ambihapathy, K.; Yalcin, T.; Leung, H.-W.; Harrison, A. G. *J. Mass Spectrom.* **1997**, *32*, 209.
(54) Vachet, R. W.; Ray, K. L.; Glish, G. L. *J. Am. Soc. Mass Spectrom.* **1998**, *9*, 341.
(55) Asano, K. G.; Goeringer, D. E.; McLuckey, S. A. *Int. J. Mass Spectrom.* **1999**, *185/186/187*, 207.
(56) Paech, K.; Jockusch, R. A.; Williams, E. R. *J. Phys. Chem. A* **2002**, *106*, 9761.
(57) Rakov, V. S.; Borisov, O. V.; Whitehouse, C. M. *J. Am. Soc. Mass Spectrom.* **2004**, *15*, 1794.
(58) Paizs, B.; Schnoelzer, M.; Suhai, S.; Young, A. B.; Harrison, A. G., manuscript in preparation.
(59) Valle, J. J.; Eyler, J. R.; Oomens, J.; Moore, D. T.; van der Meer, A. F. G.; von Helden, G.; Meijer, G.; Hendrickson, C. L.; Marshall, A. G.; Blakney, G. T. *Rev. Sci. Instrum.* **2005**, *76*, 23103.
(60) Oepts, D.; van der Meer, A. F. G.; van Amersfoort, P. W. *Infrared Phys. Technol.* **1995**, *36*, 297.
(61) Yalcin, T.; Csizmadia, I. G.; Peterson, M. B.; Harrison, A. G. *J. Am. Soc. Mass Spectrom.* **1996**, *7*, 233.
(62) Bagratashvili, V. N.; Letokov, V. S.; Makarov, A. A.; Ryabov, E. A. *Multiple Photon Infrared Laser Photophysics and Photochemistry*; Harwood: Chichester, U.K., 1985.
(63) Oomens, J.; Tielens, A. G. G. M.; Sartakov, B. G.; von Helden, G.; Meijer, G. *Astrophys. J.* **2003**, *591*, 968.
(64) Oomens, J.; Sartakov, B.; Meijer, G.; von Helden, G. *Int. J. Mass Spectrom.* **2006**, *254*, 1.
(65) Paizs, B.; Suhai, S.; Hargittai, B.; Hruby, V. J.; Somogyi, A. *Int. J. Mass Spectrom.* **2002**, *219*, 203.

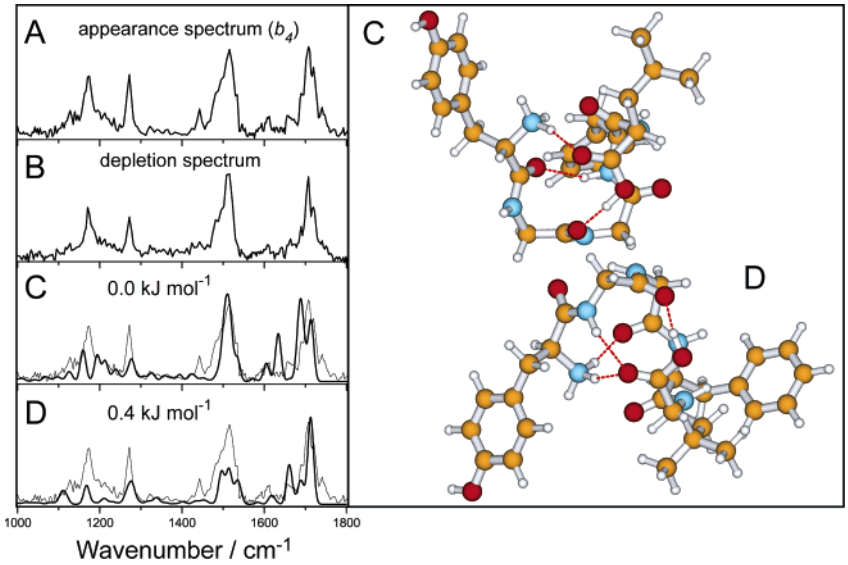

Figure 1. IR-MPD spectra of protonated Leu-enkephalin represented as (A) appearance spectrum (i.e., b_4 appearance) and (B) depletion spectrum. Comparison of the appearance spectrum (thin line) to the theoretical spectra (bold lines) for lowest-energy calculated structures (C) and (D) (relative energies indicated), showing that structure D gives a better match.

peptides was used to scan the potential energy surface (PES) of protonated Leu-enkephalin and its b_4 and a_4 fragments. These calculations started with molecular dynamics simulations on the above ions including various protonation sites using the Insight II program (Biosym Technologies, San Diego, CA) in conjunction with the AMBER force field,[67] modified in-house to enable the study of oxygen- and nitrogen-protonated amide bonds and species with C-terminal oxazolone and imine moieties.

During the dynamics calculations, we used simulated annealing techniques to produce candidate structures for further refinement, applying full geometry optimization using the AMBER force field. Special attention was paid to sampling of the conformational spaces of the cyclic b_4 and a_4 isomers. Because of the relatively small size of the rings involved (12 and 11 atoms for b_4 and a_4, respectively) and the presence of many rigid amide bonds, these species are much less flexible than their linear isomers, and the corresponding barriers to conformational changes are significantly higher than expected for linear species. Consequently, the cyclic isomers must be "heated" to higher temperatures in the simulated annealing procedure to effectively sample the entire conformational space. Simultaneously, the original trans or cis configuration of the ring amide bonds has to be constrained to avoid their isomerization during the dynamics phase of the simulated annealing. This modified sampling strategy resulted in new low-energy cyclic b_4 structures that were not available to interpret the experimental b_4 IR-MPD spectrum in our previous publication.[44] It is our experience that simulated annealing between 900 and 450 K provides extensive sampling of the conformational space of linear peptides and their fragments, whereas this range must be extended to 1400−450 K for the cyclic isomers.

The collected AMBER optimized structures were analyzed by a conformer family search program developed in Heidelberg. This program groups optimized structures into families for which the most important characteristic torsion angles of the molecule are similar. The most stable species in the families were then fully optimized at the PM3, HF/3-21G, B3LYP/6-31G(d), and finally at the B3LYP/6-31+G(d,p) levels, where the conformer families were regenerated at each level. The total energies of the lowest-energy structures are presented in Table S1 (Supporting Information). Note that for all ab initio and DFT calculations, the Gaussian set of programs was used.[68]

For the energetically most preferred protonated Leu-enkephalin structures, we have performed frequency calculations at the B3LYP/6-31G(d) level of theory. For the energetically most favored b_4 and a_4 isomers, frequency calculations at the B3LYP/6-31+G(d,p) level were carried out to produce more reliable theoretical spectra for comparison to experiment. It should be noted here that the optimized structures represent families in which the actual structures can be classified. As the ions are energetically excited, their structures are inherently dynamic and can possibly interconvert between different conformations. The relative energies are calculated by correcting the B3LYP/6-31+G(d,p) total energies for zero-point vibrational energy (ZPE) determined at B3LYP/6-31G(d). The theoretical infrared spectra were then scaled by 0.965 for the protonated Leu-enkephalin structures and 0.98 for the b_4 and a_4 structures, given the higher basis set used for the fragment structures. The stick spectra were convoluted using a 25 cm^{-1} full-width at half-maximum (fwhm) Gaussian profile to facilitate comparison with the measured IR-MPD spectra.

Results and Discussion

(1) Protonation Site of Leu-enkephalin. IR-MPD of protonated Leu-enkephalin yielded merely one observable fragment ion, b_4. The resulting IR-MPD appearance spectrum (Figure 1A) was obtained by plotting the b_4 fragment ion yield, whereas in the depletion spectrum merely the depletion in the intensity of protonated leu-enkephalin was monitored as a function of wavelength. Both spectra are essentially identical, apart from the fact that the appearance spectrum is slightly more sensitive for low-intensity bands (e.g., 1443, 1612, and 1666 cm^{-1}).

Our scan of the potential energy surface of structures for YGGFL indicates that protonation at the N-terminal amino group is more favored than protonation at amide oxygens by approximately 33.5 kJ/mol. Hence, the site of proton attachment is clearly favored on the N-terminal NH_2 group. The IR spectra of the two lowest-energy calculated conformers (Figure 1C and D) are compared to the experimental appearance spectrum, showing that the marginally higher energy structure D (+0.4

(66) Wyttenbach, T.; Paizs, B.; Barran, P.; Breci, L. A.; Liu, D.; Suhai, S.; Wysocki, V. H.; Bowers, M. T. *J. Am. Chem. Soc.* **2003**, *123*, 13768.
(67) Case, D. A.; et al. *AMBER 99*; University of California: San Francisco, CA.
(68) Frisch, M. J.; et al. *Gaussian 03*; Gaussian, Inc.: Pittsburgh, PA, 2003.

Table 1. Assignment of Calculated IR Bands for Structure D in Figure 1

expt frequency (cm^{-1})	calc frequency (cm^{-1})	intensity (km mol^{-1})	assignment
1127	1107	109	Tyr C−H in-plane bending, NH_3^+ wag
	1118	68	NH_3^+ rocking
1174	1167	91	Tyr deformation and C−O−H bending
	1169	92	Tyr deformation and C−O−H bending
	1266	86	COOH C−O−H bend and aliphatic C−H bend
1272	1277	136	N−H and C−H bend
	1280	63	Tyr deformation and C−O(H) stretch
1473	1496	210	symmetric NH_3^+ umbrella mode and N−H bend (Phe)
	1498	121	symmetric NH_3^+ umbrella and N−H bend (Leu)
	1511	118	Tyr deformation
1516	1515	259	symmetric NH_3^+ umbrella
	1532	155	amide II (N−H bend)
	1539	137	amide II (N−H bend)
1655	1660	391	antisymmetric NH_3^+ umbrella
	1683	63	antisymmetric NH_3^+ umbrella and C═O
	1690	211	amide I (C═O stretch) and antisymmetric NH_3^+ umbrella
1707	1712	782	amide I (C═O stretch)
	1716	143	amide I (C═O stretch)

kJ/mol) yields a better match. The NH_3^+ group in structure C is solvated by the Y−G and F−L amide and the COOH carbonyl oxygens and the Y aromatic side chain. In structure D, on the other hand, stabilization is provided by the G−F amide and the COOH carbonyl oxygens and the Y aromatic side chain. This difference results in a blue-shift of the antisymmetric NH_3^+ bending mode from ∼1632 (structure C) to ∼1660 cm^{-1} (structure D), thus giving an improved match for structure D. The most intense (>50 km mol^{-1}) calculated vibrational modes are summarized in Table 1, showing that the protonated NH_3^+ group is in fact involved in many relatively intense modes (e.g., ∼1500 and 1660 cm^{-1}).

The low-intensity band at 1443 cm^{-1} in the appearance spectrum could be due to the diagnostic C═O−H^+ bending mode of amide oxygen-protonated structures (see later discussion on cyclic b_4 fragment in part 2c). Given the weakness of this band, only a low number of ions are in this protonation state when the ions are at room temperature, which is consistent with the calculated energies.

(2) Fragment Ion b_4. The structure of *b* fragment ions is one of the most longstanding controversial questions in the peptide dissociation community. Scheme 1 summarizes the PFPs that lead to the formation of various b_4 isomers of protonated Leu-enkephalin. Historically, the linear acylium structure (reaction 1, Scheme 1) was proposed first,[7] but later studies showed that this structure is unstable[61,69,70] and instead a five-membered oxazolone ring is formed (reaction 2, Scheme 1) on the b_n-y_m PFP.[10] Recent computational and experimental data on protonated YAGFL-NH_2[31] indicate that the *b* structures terminated by an oxazolone ring can isomerize (reaction 3, Scheme 1) to cyclic peptides that can then, in principle, open up at any amide bond (reaction 4, Scheme 1), leading to various linear structures. For the b_4 fragment of protonated Leu-enkephalin, such ring-closure and ring-opening pathways can lead to the original $YGGF_{oxa}$ structure and isomers with permuted amino acid sequences, $GGFY_{oxa}$, $GFYG_{oxa}$, and $FYGG_{oxa}$. Note that recent computational data indicate that the cyclic b_4 structure is not formed directly from the precursor.[58]

In summary, six different b_4 isomers could be present in the mass spectrometer, the open acylium structure, $YGGF_{oxa}$, $GGFY_{oxa}$, $GFYG_{oxa}$, $FYGG_{oxa}$, and the cyclic peptide form. The last five isomers can feature various protonated forms, leading to a large number of possibilities. Experimentally, the fragment ion b_4 was generated in the ICR cell from protonated Leu-enkephalin precursor ion by applying a SORI CID pulse. The b_4 ion thus generated was interrogated with IR-MPD, yielding photofragments at *m*/*z* 120 (Phe immonium), 221 (b_2), 278 (b_3), and 397 (a_4). In the following sections (a−d), we shall discuss our spectroscopic findings in terms of the three major types of proposed fragment structures for b_4, as well as the permuted structures.

(a) Acylium Structure. As a test experiment, the *para*-aminobenzoic acid (PABA) was dissociated by CID to form the stable *para*-aminobenzoyl cation ($H_2N-C_6H_5-CO^+$) fragment, for which the IR spectrum was recorded in the range of 2100−2200 cm^{-1} (see Figure 2). The strong absorption band at 2170 cm^{-1} is attributed to the acylium CO stretch, which has in fact been reported before.[71] On the other hand, the IR photodissociation spectrum of b_4 over the spectral region of 2000−2500 cm^{-1} shows no vibrational band under identical experimental conditions. The absence of such a band in the b_4 IR spectrum clearly precludes the existence of linear acylium-type structures. This also confirms the previous hypothesis that *b* fragment acylium structures are unstable.[61,69,70]

(b) Oxazolone b_4 $YGGF_{oxa}$. In contrast to the acylium structure, where the charge is fixed, $YGGF_{oxa}$ has four possible sites of proton attachment, the N-terminus, the carbonyls O1 and O2, as well as the oxazolone ring. Calculations indicate that merely the N-terminus and the oxazolone ring are energetically accessible,[58] and hence only those structures are considered here. The experimental IR photodepletion spectrum of b_4 over the spectral range of 840−2000 cm^{-1} is shown in Figure 3A. It is immediately apparent that there are three distinct bands (1780, 1890, and 1930 cm^{-1}) at frequencies higher than usually encountered in peptides, such as the conventional amide I (CO stretching) mode of the peptide backbone (at ∼1700 cm^{-1}) and the carboxylic acid CO stretch (at ∼1750 cm^{-1}).[37,40] This indicates that a new chemical moiety must have been formed in the CID process, which is not present in linear peptides. All three bands can be ascribed to CO stretching modes of the oxazolone structures B, C, and E (see Figures 3 and 4), as shown in a previous publication.[44] Differences in the chemical environment lead to significant differences in the CO stretching frequency of the oxazolone ring. When the proton is located at the N-terminus and the oxazolone CO is hydrogen-bonded to it (structure B), the observed CO frequency is as low as 1780 cm^{-1}. Conversely, when the proton is attached to the oxazolone ring and the oxazolone CO is not hydrogen-bonded, the observed CO frequency appears at 1930 cm^{-1} (structure C), which is a substantial 150 cm^{-1} higher than for structure B. The last

(69) Yalcin, T.; Khouw, C.; Csizmadia, I. G.; Peterson, M. R.; Harrison, A. G. *J. Am. Soc. Mass Spectrom.* **1995**, *6*, 1165.
(70) Paizs, B.; Szlavik, Z.; Lendvay, G.; Vekey, K.; Suhai, S. *Rapid Commun. Mass Spectrom.* **2000**, *14*, 746.
(71) (a) Oomens, J.; Bakker, J. M.; Sartakov, B.; Meijer, G.; von Helden, G. *Chem. Phys. Lett.* **2003**, *367*, 576. (b) Oomens, J.; Moore, D. T.; Meijer, G.; von Helden, G. *Phys. Chem. Chem. Phys.* **2004**, *6*, 710.

Scheme 1. Dissociation of Singly Protonated Leu-enkephalin (A) Shown Schematically in Amino Acid Three-Letter Code, and (B) Shown Mechanistically for Four Proposed Peptide Fragmentation Pathways (PFP's), Yielding (1) Linear Acylium, (2) Linear Oxazolone Terminated Structures, (3) Isomerization of the Linear Oxazolone Terminated Structure Can Give Rise to the Cyclic Isomer, and (4) Re-opening of the Cyclic Structure Can Then Lead to a Range of Oxazolone Structures, with Either the Original Amino Acid Sequence or Permuted Sequences

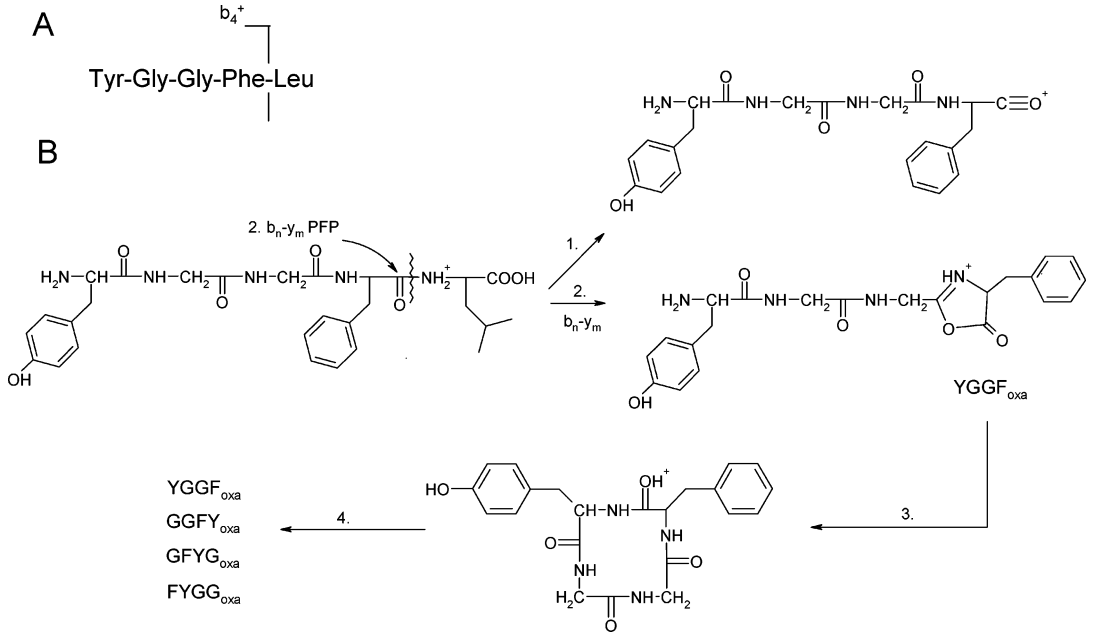

remaining band at 1890 cm^{-1} is well-matched by the calculated oxazolone CO stretch for structure E, where proton attachment occurs on the N-terminus, but the oxazolone CO is not hydrogen-bonded. Although band intensities are not always as reliable in IR-MPD as in linear absorption techniques, the relative band intensities appear to reflect the relative stabilities of these oxazolone structures; that is, the N-terminal amino-protonated B structure is significantly more abundant than the oxazolone-protonated C. The fact that the N-terminus competes as a site of protonation shows that the oxazolone ring is not always as basic as is commonly suggested in the literature.[61,72,73]

The remainder of the IR spectrum agrees reasonably well with a mixture of structures B, C, and E, with the notable exception of the band at 1440 cm^{-1} (erroneously ascribed in our previous communication as the 1420 cm^{-1} band),[44] which is much more prominent in the experimental spectrum than was predicted for these structures.

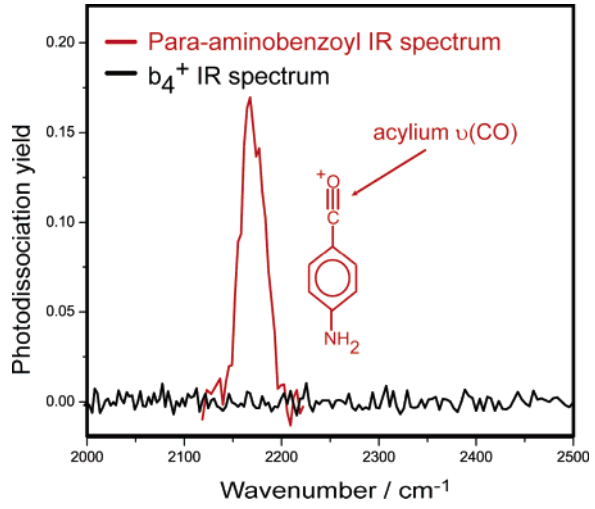

Figure 2. Experimental IR spectra of the *para*-aminobenzoyl cation (red) and the CID product ion b_4 of Leu-enkephalin (black) over the spectral range from 2000 to 2500 cm^{-1} under identical experimental conditions, clearly showing the acylium CO stretch of the *para*-aminobenzoyl cation at ~2170 cm^{-1}. Conversely, no such band is observed for b_4, thus excluding the linear acylium-type fragment structures (Scheme 1, reaction 1).

(c) Cyclic b_4 Structures. The oxazolone $YGGF_{oxa}$ structure can isomerize to the cyclic structure (Scheme 1, reaction 3). The most basic site for this structure is one of the amide oxygens, as no free N-terminal amine group is available. In principle, amide O protonation can be distinguished from other proton attachment sites by its characteristic C═O−H^+ bending mode. However, in our previous paper,[44] the energetically most favored cyclic peptide structure did not match the b_4 experimental spectrum convincingly. In light of the recent *b* ion cyclization mechanism,[31] we have performed an even more detailed scan (described in detail in the Computational Details section) of the cyclic *b* isomers and found new structures that are energetically more favored than our previous candidate. One of those structures (structure D, Figure 4) is protonated at the Phe−Tyr amide oxygen, and its relative energy is 15.4 kJ/mol higher than the N-terminal-protonated $YGGF_{oxa}$.

The calculated IR spectrum of structure D shows a medium-intensity band at ~1440 cm^{-1}, due to the diagnostic C═O−H^+ bending mode, which gives a convincing match for the unassigned band in the b_4 experimental spectrum. While not all cyclic structures give such a good agreement, the cyclic structures consistently predict the C═O−H^+ bending mode in the range from 1400 to 1450 cm^{-1}. It appears that the DFT-predicted C═O−H^+ bending mode frequency is strongly dependent on the exact conformation of the cyclic structure, and this explains our initial non-assignment of the 1440 cm^{-1} band.[44] Another argument in favor of the cyclic structure is the fact that this structure could rationalize the stronger-than-

(72) Polce, M. J.; Ren, D.; Wesdemiotis, C. *J. Mass Spectrom.* **2000**, *35*, 1391.
(73) Rodriquez, C. F.; Shoeib, T.; Chu, I. K.; Siu, K. W. M.; Hopkinson, A. C. *J. Phys. Chem. A* **2000**, *104*, 5335.

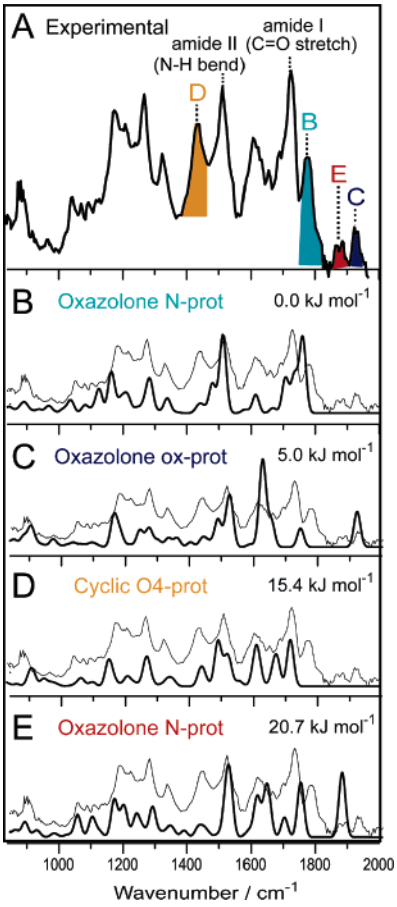

Figure 3. (A) Experimental IR spectrum of b_4 as compared to calculated IR spectra for (B) N-terminal-protonated oxazolone structure, (C) oxazolone ring-protonated oxazolone structure, (D) cyclic peptide structure protonated on O4, and (E) N-terminal-protonated oxazolone structure (theoretical spectra indicated by bold lines). The relative energies of the structures are given. The assignment of the oxazolone CO stretching modes and cyclic structure C═O−H$^+$ bending modes is depicted in color-coding in the experimental spectrum. The corresponding structures are shown in Figure 4. Note that none of the oxazolone structures can account for the relatively intense experimental band at 1440 cm^{-1}.

expected amide I band at 1700 cm^{-1}, which is underrepresented by the theoretical spectra for the oxazolone structures B, C, and E. This shows that a mixture of oxazolone and cyclic structures is formed. Nonetheless, it is difficult to establish the relative abundances of each structure from the IR spectrum, especially because the vibrational bands for both types of structures display substantial overlap.

(d) Permuted Oxazolone Structures. As the cyclic structures appear to be formed, this raises the possibility of permuted oxazolone structures as the cyclic structure opens up (Scheme 1, reaction 4). The IR spectra neither provide evidence in favor nor against the existence of these structures (not shown). Nonetheless, the calculations predict differences in the relative energetics of proton attachment for the N-terminus relative to the oxazolone ring (see Figure S1, Supporting Information). Notably for $GGFY_{oxa}$ and $GFYG_{oxa}$, proton attachment at the oxazolone ring is energetically favored as compared to the N-terminus, while for $FYGG_{oxa}$, protonation at the N-terminus is more preferred similarly to $YGGF_{oxa}$. While the calculated IR spectra do not allow us to directly differentiate between oxazolone structures with the original amino acid sequence (i.e., $YGGF_{oxa}$) and permuted b_4 structures, the $GGFY_{oxa}$ and

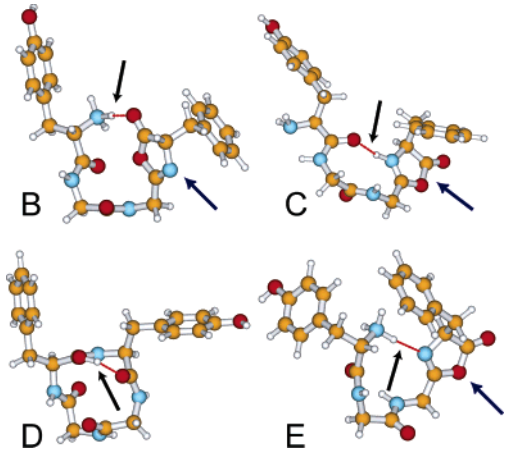

Figure 4. Structures corresponding to the theoretical spectra shown in Figure 3, showing sites of proton solvation (black arrows) and oxazolone rings (blue arrows).

$GFYG_{oxa}$ permuted structures cannot be present in substantial amount, otherwise the intensity of the CO stretch at 1930 cm^{-1}, linked to the oxazolone-protonated structure, should be much higher. Note that this argument does not apply to the permuted $FYGG_{oxa}$ structure, where the N-terminus is also the favored site of proton attachment. It is also worth noting here that the oxazolone-protonated $GGFY_{oxa}$ isomer is energetically the most favored among the linear b_4 isomers (Figure S1, Supporting Information). In separate MS^3 experiments of b_4 of protonated Leu-enkephalin, it has been shown that only a small fraction of the ion population in a Q-TOF type instrument are present as $GGFY_{oxa}$.[58] This suggests that "scrambling" pathways are not the major reaction channels for the b_4 ion of Leu-enkephalin in the Q-TOF, which is surprising, given the apparently significant abundance of cyclic b_4 structures in our FT-ICR instrument. This contradiction can be resolved by considering the relatively long time-scale of the latter experiment that clearly favors rearrangements occurring on the scrambling PFPs.

(e) Evidence for the Proton Mobility between Two Sites. In CID of protonated peptides, the internal energy of the peptide is increased, leading to a mobile proton that induces charge-directed dissociation.[11,12] The b_n-y_m PFP's[10] are believed to give rise to N-terminal linear b fragments with an oxazolone ring ($YGGF_{oxa}$ for the b_4-y_1 pathway of YGGFL), which are for a short period bound to the C-terminal fragment (Leu for YGGFL). In the thus formed proton-bound dimer, the N- and C-terminal fragments compete for the extra proton before the complex falls apart. Given the much higher proton affinity (PA) of the oxazolone fragment (978.2 kJ/mol) as compared to Leu (909.2 kJ/mol), the former displays exclusive retention of the proton on the oxazolone ring nitrogen (see Scheme 2). As the N-terminus is an energetically more favorable site of proton attachment for $YGGF_{oxa}$, one would expect to observe a gradual conversion of oxazolone-protonated to N-terminally protonated structures.

In these experiments, the ions are left to cool to room temperature following SORI CID by leaving a radiative emission delay prior to spectroscopic probing; previous experiments showed that an approximate temperature of 600−800 K was necessary to induce CID of this peptide.[49] Figure 5 shows the IR photodepletion spectra recorded after two different radiative cooling delays: 0.5 and 4 s. It can clearly be seen that the

Scheme 2. Schematic Showing the Main b_n-y_m PFP Product from Protonated Leu-enkephalin (See Figure 2), Where the N-terminal b_4 Oxazolone Fragment Is Proton-Bound to the C-terminal Leu Fragment, the Oxazolone Fragment Exclusively Retains the Proton, Due to Its Higher Proton Affinity (PA). The Proton Is Then Transferred to the N-terminus, Which Is the Highest PA Site

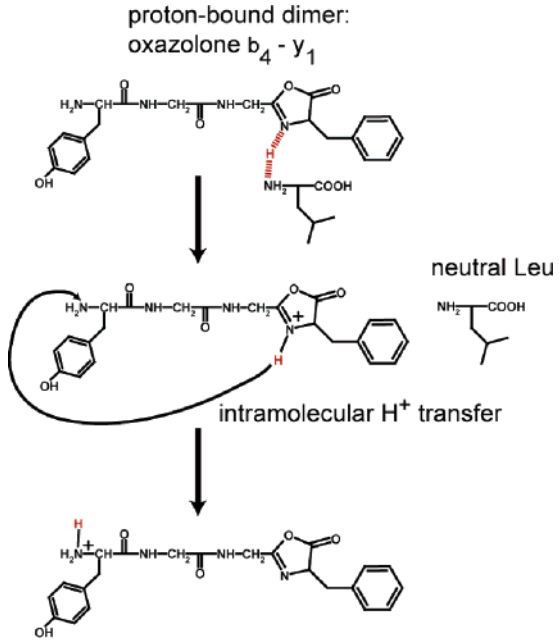

intensity of the 1930 cm^{-1} band (navy color), associated with the oxazolone-protonated structure (structure C, see Figure 4), is noticeably reduced after a cooling delay of 4 s, while this band is quite prominent for a delay of merely 0.5 s. On the other hand, the 1780 cm^{-1} band (cyan) remains the most intense oxazolone CO stretching feature, and even appears to slightly increase in intensity upon increasing the delay time to 4 s (although this is more difficult to establish than the decrease in the navy band). Note that the band at 1890 cm^{-1} (red) is much weaker, and hence none of the oxazolone-protonated structures are irreversibly converted into this higher-energy conformation. This suggests that a net proton transfer takes place from the oxazolone ring to the energetically more favorable N-terminus. The reason why a significant amount of the ion population is originally in the energetically less favorable oxazolone-protonated form could be rationalized by the mechanistic pathway in Scheme 2, where it is assumed that the proton is exclusively located on the oxazolone ring nitrogen after the proton-bound b_4-y_1 dimer separates.

When the FELIX wavelength was set to a fixed wavelength of 5.2 μm (~1930 cm^{-1}), corresponding to the band center of the oxazolone CO stretch in the oxazolone-protonated structures, the yield of the main photodissociation product of b_4, a_4, is characterized by a smooth falloff on a time-scale of seconds, which is adequately fitted by an exponential decay function (see inset of Figure 5B). Such a decrease is consistent with a progressive depletion of structure C due to radiative cooling, which is expected to be the main cooling pathway under these pressure conditions (~2×10^{-7} mbar).[74]

It should be noted though that the measurements in Figure 5 are mainly intended for establishing qualitative trends and not for determining proton-transfer kinetics in the ion population.

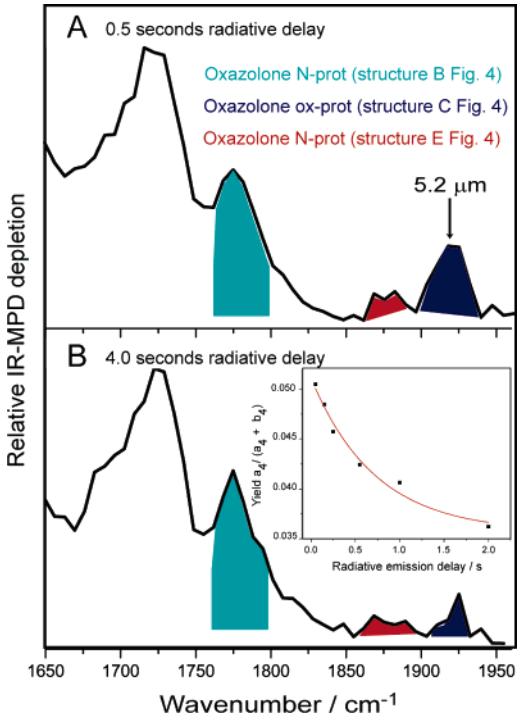

Figure 5. IR photodepletion spectrum of the fragment ion b_4 after radiative cooling delays of (A) 0.5 s and (B) 4 s. The structural assignment of the oxazolone CO stretching bands is depicted in color-coding. The inset in (B) shows the photodissociation yield of a_4 following irradiation of b_4 at a fixed wavelength of 5.2 μm (~1930 cm^{-1}) for various radiative cooling delays; an exponential decay function is fitted to the photodissociation yield (i.e., appearance of a_4).

The time-scale of the SORI CID experiment is on the order of seconds, and hence not every b_4 fragment ion is formed at the same time. Given these long delays, it is not surprising that most proton transfer from the oxazolone nitrogen to the N-terminus would already have taken place by the time the IR spectra are recorded. To answer whether all b_4 fragment ions are initially protonated on the oxazolone ring nitrogen, as suggested in Scheme 2, would require a much faster experiment, which is beyond the scope of this study.

As the calculated energy difference between the lowest-energy N-terminal-protonated and oxazolone-protonated structures is merely 5 kJ mol^{-1} (which lies within 2 kT,) an observable proportion (i.e., >10%) of the ion population should remain in the energetically less favorable oxazolone-protonated structure. This is confirmed by the experimental findings, showing that the intensity of the 1930 cm^{-1} band does not reach zero even after 4 s radiative cooling delay (which is a longer delay, as some b_4 ions may be formed toward the beginning of the SORI pulse). While the proton mobility in peptides had already been demonstrated experimentally by a combined H/D exchange and peptide dissociation study,[23] this is in fact the first time that the proton mobility between two attachment sites can be directly monitored in the gas phase. Given the importance of the mobile proton in the CID process, this gives interesting insight into the dissociation chemistry of protonated peptides.

(f) Proton-Transfer Pathway. A careful inspection of structures B, C, and E (Figure 4) shows that b_4 ions undergo not only intramolecular proton transfer but also major structural changes. All of these structures are stabilized by strong H-bonds, which connect the N- and C-termini and lead to conformers

(74) Dunbar, R. C. *Mass Spectrom. Rev.* **2004**, *23*, 127.

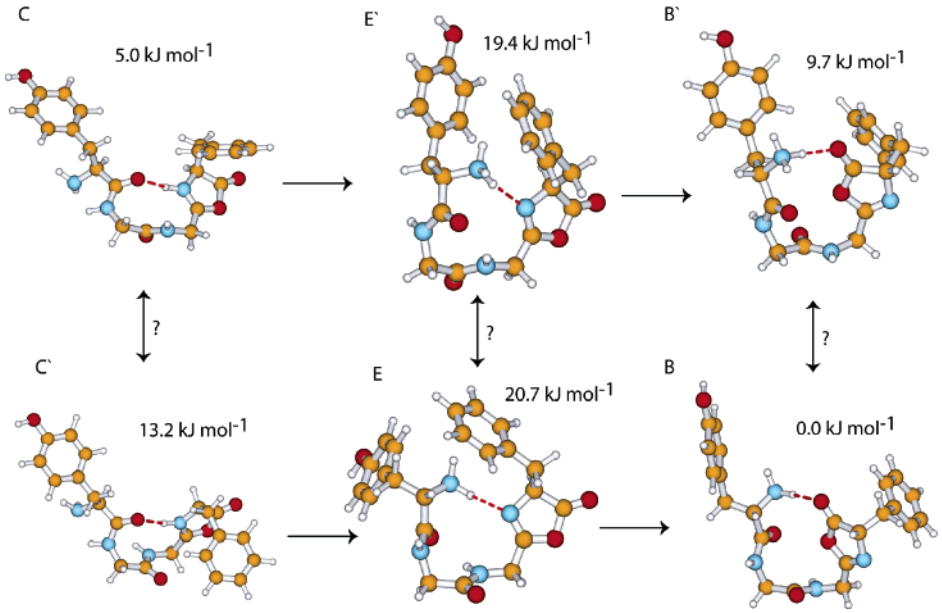

Figure 6. Schematic showing how the proton transfer from the oxazolone ring (structure C or C′) to the N-terminus (structure B or B′) can be rationalized by interconversion via structures E or E′. Note that the upper structures are folded anticlockwise, whereas the structures below are folded clockwise. Interconversion between these folding conformations is more complicated, and no obvious pathway has been found. The relative energies of the structures are given.

Scheme 3. Schematic for Mechanisms of a_4 Ion Formation from b_4, as Well as a_4 Ion Cyclization

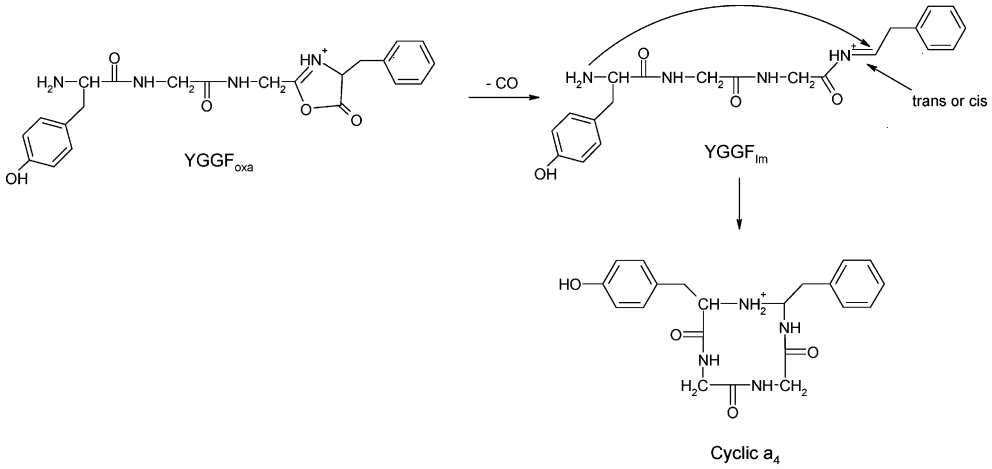

featuring large intramolecular rings. Such structures can be folded clockwise or anticlockwise. Structures B and E belong to the former group, while species C belongs to the latter class. It is worth noting here that for each structure oppositely folded conformers (B′, C′, and E′) exist, as depicted in Figure 6. The energetically most favored b_4-y_1 transition state (TS)[58] leaves an oxazolone-protonated structure behind that is very similar and can rapidly isomerize to species C. However, we cannot exclude formation of C′-type oxazolone-protonated structures based on the available experimental and theoretical data. (The theoretical IR spectra for the C−C′, B−B′, and E−E′ pairs are very similar to one another and do not allow one to distinguish the oppositely folded structures experimentally.) Structures C and C′ must undergo two major changes to transform to B and B′ including transfer of the added proton and rotation of the C-terminal oxazolone ring. It is very likely that proton transfer to the N-terminal amino group occurs first, and this step is followed by rotation of the oxazolone ring. Structures E and E′ play a critical role during this transition because these species are already protonated at the amino group while the oxazolone ring is not rotated yet. This is the first experimental evidence for such an intermediate structure on the proton-transfer pathway, which is probably only observed as some ions are kinetically stabilized in this structure. It is likely that we observe species E and/or E′ merely because the transition between C and B is a rather complicated multistep process with substantial barriers that are due to the breaking of strong H-bonds. Moreover, the complexity of this transition is probably responsible for the long time-scale of the overall process and allows for the monitoring of the proton-transfer process described above on the ∼seconds time-scale.

(3) Fragment Ion a_4. In our experiments, a_4 ions are mainly formed from oxazolone-protonated b_4 species ($b_4 \rightarrow a_4$ PFP).[10,70] CO can be expelled from the parent ion "above" and "below" the plane of the oxazolone ring, leading to trans or cis imines in the corresponding a_4 species (Scheme 3). Similarly to various

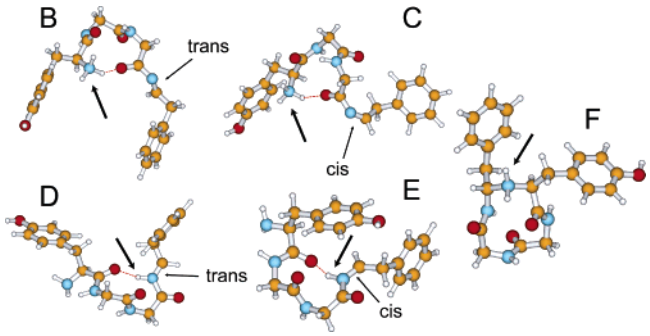

Figure 7. Lowest-energy structures for a_4 fragment structures: (B) imine trans N-terminal-protonated, (C) imine cis N-terminal-protonated, (D) imine trans imine-protonated, (E) imine cis imine-protonated, and (F) cyclic N-protonated (D_Phe), for which the IR spectra are shown in Figure 8.

b_2 ions,[70] the barrier to formation of the trans form (129.2 kJ/mol) is lower than the barrier to the cis form (144.7 kJ/mol) for $YGGF_{oxa}$.[58]

Besides the Y−G and G−G amide bonds, the a_4 ion ($YGGF_{im}$) features the C-terminal −CO−N═C moiety. The latter can quite freely rotate around the CO−N bond (single bond character), while the −N═C− imine bond is fixed to the trans or cis isomers depending on the $b_4 \rightarrow a_4$ TS in which the particular a_4 species is formed (see above). The conformational spaces of the N-terminal amino, amide oxygen, and C-terminal imine-protonated forms were carefully scanned[58] considering both the trans and the cis imine isomerization states. These calculations indicated that the N-terminal amino group is the energetically most favored protonation site, while protonation at the C-terminal imine is 8 kJ/mol higher in energy. For both the amino- and the imine-protonated forms, the trans imine isomerization state is favored with respect to cis. All but one of the amide oxygen-protonated forms of a_4 are energetically much less favored[58] and will not be discussed in detail in the present paper.

Similarly to the $YGGF_{oxa}$ b_4 species, the energetically most favored $YGGF_{im}$ structures feature strong H-bonds that connect C- and N-terminal functionalities. In such geometrical arrangements, the N-terminal amino group can attack (Scheme 3) the carbon center of the protonated imine group, forming a cyclic isomer of a_4. Scanning of the conformational spaces of cyclic a_4 ions resulted in two structures (D_Phe and L_Phe (Figure S2, Supporting Information)) that are energetically as favored (relative energy at −0.3 and 0.1 kJ/mol, respectively) as the most stable $YGGF_{im}$ species.

The a_4 fragment ion was generated in slightly more energetic SORI conditions and simultaneous SORI on b_4. The photodissociation of a_4 gave rise to fragment ions at m/z 380 (a_4-NH_3) and 278 (b_3). In the following two sections, we shall discuss our spectroscopic findings in terms of the two major types of proposed fragment structures (i.e., linear and cyclic) for a_4.

(a) Linear Imine a_4 Structures. As discussed above, there are a large number of putative structures for a_4, thus making the interpretation of the IR spectrum potentially much more difficult than in the case of b_4. The experimental IR spectrum in Figure 8 is compared to four distinct linear imine-type structures: the amino-protonated structures B (trans) and C (cis), as well as the imine-protonated structures D (trans) and E (cis). There are clear differences in the calculated IR spectra that allow these chemical structural differences to be distinguished. Moving

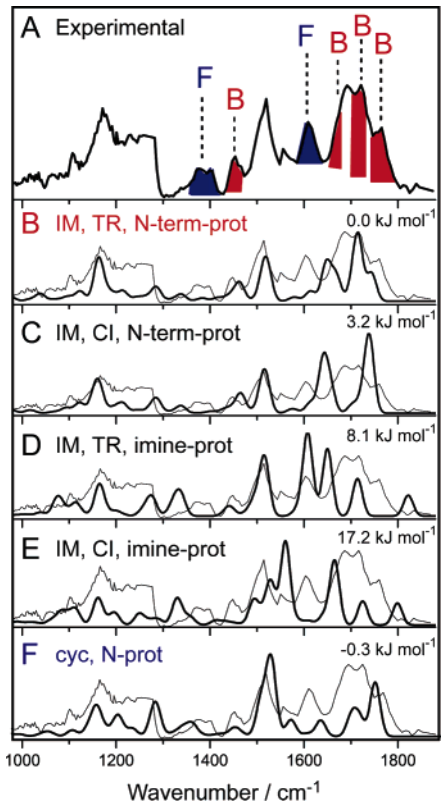

Figure 8. (A) IR photodepletion spectrum of the fragment ion a_4, as compared to the calculated spectra (bold lines) for (B) imine trans N-terminal-protonated, (C) imine cis N-terminal-protonated, (D) imine trans imine-protonated, (E) imine cis imine-protonated, and (F) cyclic N-protonated, which are shown in Figure 7. The identification of structures B and F is depicted in color-coding.

the proton from the N-terminus to the imine N, for example, results in a blue-shift of the diagnostic imine CO stretch from ~1650 cm^{-1} (structure B) to 1820 cm^{-1} (structure D). The absence of a band >1800 cm^{-1} clearly precludes the presence of the imine group as a site of proton attachment (and thus of structures D and E), whereas the red side of the relatively broad 1700 cm^{-1} band is consistent with the presence of structure B (color-coded in red in Figure 8). In fact, the broad band from ~1650−1800 cm^{-1} can be well explained by structure B, as the strong C═N stretch at 1714 cm^{-1} coincides with the maximum absorption of this band and even the shoulder to the blue is reproduced (both color-coded in red). Moreover, the remainder of the calculated spectrum for structure B matches most of the experimental features, and it is apparent that structure B gives a much better match to the experimental spectrum than any of the other imine-type structures (i.e., C, D, or E).

The absence of imine-protonated structures (i.e., structures D and E) is surprising, as this site is commonly believed to be more basic than the N-terminus.[52] Moreover, in the case of b_4, it was possible to observe a mixture of structures with different sites of protonation. (As shown in Scheme 3, a_4 ions are formed on the $b_4 \rightarrow a_4$ PFP as imine-protonated species.) This suggests that the proton transfer is much faster in the case of imine-type a_4 fragments than in the case of oxazolone-type b_4 structures. This is likely due to the fact that the −CO−N═C moiety in the former is rather flexible while rotation of the oxazolone ring of the latter is more hindered. It is worth noting here that the H-bond-stabilized macro-rings of structures B and D are

similarly folded (Figure 7), thus facilitating the proton transfer from the C- to the N-terminus.

While imine-protonated structures can be conveniently excluded on the basis of the absence of an imine CO band >1800 cm^{-1}, the case is not quite as clear-cut for the cis imine structure protonated on the N-terminus (structure C). The main difference here as compared to structure B is a red-shift of the imine CO stretch to ~1640 cm^{-1} and a less convincing match to the main absorption band around 1700 cm^{-1} and in particular the shoulder to the blue. We therefore conclude that some structure C may be formed, but that structure B, with a trans imine bond, is the predominant imine-type structure generated. This shows that an insight can be gained on the dynamics of the $b_4 \rightarrow a_4$ PFP.

(b) Cyclic a_4 Structures. Despite the relatively clear picture for the imine-type structures, there are two experimental bands that are not reproduced by structure B, the bands around 1380 and 1600 cm^{-1}. The appearance of these bands can be rationalized with cyclic structures (Figure 8F). In fact, two cyclic structures were found, D_Phe and L_Phe (Figure S2, Supporting Information), which differ from one another in the stereochemistry of the Phe α-carbon. That is, D_Phe and L_Phe correspond to the D and L configurations, respectively. It is worth noting here that the energetically slightly more favored D_Phe structure is formed from trans linear a_4 species, while L_Phe can be derived only from cis linear a_4 structures. The most favorable site of proton attachment in structures D_Phe and L_Phe is the N atom, which previously was the N-terminus of the imine structure. This ammonium-type structure has two chemically diagnostic bands: the out-of-plane bending mode of the NH_2^+ group at ~1390 cm^{-1} and the scissoring mode of this group at ~1600 cm^{-1}. These two modes match the previously unassigned bands, while also not contradicting the remainder of the experimental spectrum. While L_Phe appears to give a better match (Figure S2, Supporting Information), both theoretical spectra are fairly similar, and neither structure can be excluded.

We therefore conclude that there is a mixture of linear (predominantly trans) amino-protonated imine structures and cyclic a_4 structures. This picture is very similar to the case of b_4, where also a mixture of linear and cyclic structures is observed. It is worth noting that the cyclic a_4 isomer can open up at amide bonds on b_n-y_m like PFP's after proton transfer. Such reactions can lead to the formation of new linear isomers that can fragment further to produce non-direct sequence ions.[31] The related chemistry will be investigated in a forthcoming publication.[58]

Conclusions

This work demonstrates the important structural information on peptides and their dissociation products that can be gained from IR spectroscopy in combination with theoretical studies, including the site(s) of protonation and the chemical rearrangements that have taken place. Thus, it is confirmed that the b_4 fragment forms a mixture of linear oxazolone and cyclic structures, while the a_4 fragment forms a mixture of linear imine and cyclic structures. Moreover, the site of proton attachment and for b_4 even the dynamics of intramolecular proton transfer in the ion population can be followed by comparing the relative intensities of the oxazolone CO stretch bands for varying time delays. This gives qualitative insight into the mobility of the proton, which plays a crucial role in peptide dissociation and which so far has been difficult to ascertain with other gas-phase structural techniques. The proton-transfer kinetics in a_4 appeared to occur on a faster time-scale than in b_4, due to the more flexible backbone of a_4, and could hence not be followed in this experiment.

The experimental results can be well explained with the pathways in the competition (PIC) peptide fragmentation model. In terms of furthering the understanding of peptide dissociation chemistry, the combined approach of computational modeling and IR spectroscopy is particularly beneficial. The calculations require experimental techniques that can benchmark some of the predictions. By analogy, IR spectroscopy relies on comparison to calculated structures/spectra to interpret the results. It is expected that the combined modeling−spectroscopy approach can address many of the open questions in the field of peptide dissociation, such as whether *b* fragment ions adopt linear oxazolone or cyclic structures, or in fact mixtures as observed here. These results suggest that formation of the cyclic structures is more common than previously thought, which presents possible challenges for the sequencing of amino acids in tandem MS. The fundamental study of these processes should lead to an eventual semiquantitative prediction of the main PFP's in CID of protonated peptides and hence enhance the structural information that can be obtained from tandem mass spectra.

Acknowledgment. This work is financially supported by the "Nederlandse Organisatie voor Wetenschappelijk Onderzoek" (NWO) and the Deutsche Forschungsgemeinschaft (SU 244/3-1). The skillful assistance by the FELIX staff is gratefully acknowledged, and in particular that by Drs. Britta Redlich and Lex van der Meer. Construction and shipping of the instrument was made possible with funding from the National High Field FT-ICR Facility (grant #CHE-9909502) at the National High Magnetic Field Laboratory, Tallahassee, FL. We thank Professors John R. Eyler and Alan G. Marshall for their collaboration with the FT-ICR project. The DFT-calculated structures were rendered by Molden to allow their visualization.

Supporting Information Available: Table S1 and Figures S1 and S2, as well as complete refs 67 and 68. This material is available free of charge via the Internet at http://pubs.acs.org.

JA068014D